Structural, Mechanical and Swelling Characteristics of 3D Scaffolds from Chitosan-Agarose blends

Reda M. Felfel[1,2*], Mark J. Gideon-Adeniyi[1], Kazi M. Zakir Hossain[1], George A. F. Roberts[1], David M. Grant[1]

[1]Advanced Materials Research Group, Faculty of Engineering, University of Nottingham, UK

[2]Physics Department, Faculty of Science, Mansoura University, Egypt

Abstract

This study aimed to explore the correlation between mechanical and structural properties of chitosan-agarose blend (Ch-Agrs) scaffolds. Porosity of Ch-Agrs scaffolds was constant at 93%, whilst pore sizes varied between 150 and 550 µm. Pore sizes of the blend scaffolds (150 - 300 µm) were significantly smaller than for either agarose or chitosan scaffolds alone (*ca.* 500 µm). Ch50-Agrs50 blend scaffold showed the highest compressive modulus and strength values (4.5 ± 0.4 and 0.35 ± 0.03 MPa) due to reduction in the pore size. The presence of agarose improved the stability of the blends in aqueous media. The increase in compressive properties and residual weight after the TGA test, combined with the reduction in the swelling percentage of the blend scaffolds suggested an interaction between chitosan and agarose via hydrogen bonding which was confirmed using FTIR analysis. All wet blend scaffolds exhibited instant recovery after full compression. This study shows the potential of Ch-Agrs scaffolds for repairing soft tissue.

Keywords: Chitosan; Agarose; Blend scaffolds; Compressive properties; Recovery; Pore size.

1   Introduction

Different biopolymers have been investigated to form three-dimensional (3D) porous constructs, such as scaffolds, for tissue engineering applications (Alina Sionkowska, 2011). Typical material selection criteria include: having a highly porous structure; be made from biodegradable materials; have a surface chemistry conducive for cellular attachment, proliferation and differentiation; adequate structural integrity for the application loading in order to withstand collapsing pores; be cytocompatible and easily fabricated; moulded or shaped into the desired morphology (Jayakumar, Menon, Manzoor, Nair, & Tamura, 2010; Sachlos & Czernuszka, 2003). Over the past few years, there has been more focus on blending different types of polymers in order to be able to have structures that exhibit the required cellular response and improved mechanical properties as opposed to single constituents (Alina Sionkowska, 2011).

Both synthetic and natural biopolymers have been utilised as 3D porous scaffolds for different biomedical applications (Alina Sionkowska, 2011). Natural polymers such as chitosan, collagen and gelatine have demonstrated superior cell adhesion and proliferation over synthetic counterparts due to their similarity to extracellular matrix material (Mano *et al.*, 2007; Zhu & Marchant, 2011). Out of all the natural biopolymers, chitosan has potential advantages for regeneration of cartilage tissue as a result of its similarity to glycosaminoglycans, a component of cartilage matrix (Ragetly, Slavik, Cunningham, Schaeffer, & Griffon, 2010). Chitosan is a polysaccharide produced by deacetylation of natural chitin, which is abundantly available in the shells of arthropods and cell walls of fungi (Elieh-Ali-Komi & Hamblin, 2016). Chitosan is a biocompatible and biodegradable copolymer of glucosamine and N-acetyl-glucosamine (Elieh-Ali-Komi & Hamblin, 2016) and is soluble in dilute acidic aqueous media (i.e. water containing small fraction of acids such as acetic acid or hydrochloric acid) (Elieh-Ali-Komi & Hamblin, 2016). Water absorption and swelling, and hence loss of mechanical strength and integrity have been the main limitations to the use of plain chitosan as an implant. Consequently, physical and chemical crosslinkers have been introduced to enhance its stability in aqueous environments (Szymańska & Winnicka, 2015). Another approach that has been proposed is the blending with synthetic or natural polymers to control not only the swelling, but also to improve the mechanical performance (A. Sionkowska *et al.*, 2014; Doulabi, Mequanint, & Mohammadi, 2014; El-hefian, Nasef, & Yahaya, 2012; Grohens, Thomas, & Jyotishkumar, 2015; Teng, Wang, & Kim, 2009). Chitosan is able to form hydrogen bonds with other polymers because of the presence of the -OH and –NH$_2$ polar groups (Chaudhary, Vadodariya, Nataraj, & Meena, 2015; Trivedi, Rao, & Kumar, 2014). For example, chitosan-silk fibroin blends were investigated for possible applications in cosmetic science (A. Sionkowska *et al.*, 2014). Chitosan has also been successfully

blended with various natural and synthetic biopolymers such as alginate, collagen, hyaluronic acid, agarose, cellulose, starch, gelatine, polycaprolactone, polylactic acid and polyvinyl alcohol (A. Sionkowska *et al.*, 2014; Amir Afshar & Ghaee, 2016; Lewandowska, Sionkowska, & Grabska, 2015; Li, Ramay, Hauch, Xiao, & Zhang, 2005; Sarasam & Madihally, 2005; Shanmugasundaram *et al.*, 2001; A. Sionkowska, Wisniewski, Skopinska, Kennedy, & Wess, 2004; Szymańska & Winnicka, 2015; Wan, Wu, Yu, & Wen, 2006).

Agarose is another biocompatible polysaccharide polymer and is obtained from seaweed (Bhat & Kumar, 2012; Hu *et al.*, 2016). A stiff hydrogel can be prepared from agarose at low concentrations (1wt%) making it useful for blending with other polysaccharides to enhance their stability in aqueous media (Cao, Gilbert, & He, 2009). The stiffness of agarose can be easily tuned by using different agarose to water concentrations to suit the end application either in the form of hydrogels or scaffolds (Cao, Gilbert, & He, 2009). Therefore agarose has been investigated for a wide range of biomedical applications such as wound healing, cartilage repair and regeneration of neural tissue (Bhat & Kumar, 2012; Bhat, Tripathi, & Kumar, 2010; Cao, Gilbert, & He, 2009; Stokols & Tuszynski, 2006; Tripathi & Melo, 2015). However, the lack of cell adhesion is a drawback for agarose (Cao, Gilbert, & He, 2009), consequently, combining agarose with other biopolymers such as chitosan is crucial to improve the cell attachment.

The similarity in the chemical structures of chitosan and agarose have led to investigations of chitosan-agarose-blends as potential candidates for biomedical applications such as skin regeneration, neural tissue, liver tissue model, cartilage and bone repair (Bhat & Kumar, 2012; Bhat, Tripathi, & Kumar, 2010; Cao, Gilbert, & He, 2009; Stokols & Tuszynski, 2006; Tripathi & Melo, 2015; Trivedi, Rao, & Kumar, 2014). The cytocompatibility, genotoxicity, in vitro and in vivo responses of their blends have been studied in hydrogel and scaffold forms (Bhat & Kumar, 2012; Cao, Gilbert, & He, 2009; Merlin Rajesh Lal, Suraishkumar, & Nair, 2017; Teng, Wang, & Kim, 2009; Trivedi, Rao, & Kumar, 2014; Zamora-Mora, Velasco, Hernández, Mijangos, & Kumacheva, 2014). However, the mechanical and physical performance of chitosan-agarose blend scaffolds have not been fully investigated. Furthermore, since the mechanical performance plays a crucial role in the selection of biomaterials for production of implants, the compressive properties of different ratios of chitosan-agarose blends were investigated in this study under dry and wet conditions along with swelling, thermal and structural characteristics.

2   Materials and Methods

2.1   Materials

Chitosan powder (Mw 471 kDa) of 84% degree of deacetylation was purchased from Weifeng Kenai Ltd, China. Electran® Agarose powder (DNA Grade, Mw ~ 120,000 Da, density 1.64 g.cm^{-3}) from VWR international ltd (UK) was used in this study. Gelling and melting temperature ranges of this type of agarose are 34-37°C and 60-90°C respectively. Glacial acetic acid from Sigma Aldrich (UK) was also used.

2.2   Preparation of 3D blend scaffolds

Chitosan solution (2 wt%) was prepared by dissolving 1 g of chitosan powder at room temperature in 50 ml deionised water containing 1.25 ml acetic acid with vigorous stirring (500 rpm) for 15 min. The chitosan solution was then covered with cling film and left overnight to eliminate air bubbles. A 2 wt% agarose solution was also prepared by heating 1 g of agarose powder in 50 ml deionised water at 95 °C for 15 min using a hot plate magnetic stirrer until a fully dissolved and a clear solution was obtained. To prepare the blend scaffolds, a predetermined amount of chitosan solution (based on the required composition, see Table 1) was added slowly to the agarose solution at 95°C with continuous vigorous stirring (500 rpm) for 30 min until a uniform solution was obtained. Chitosan, agarose and their blend solutions were cast in a PTFE mould (10 mm diameter and 10 mm height) and left to cool down to room temperature (for agarose containing samples) before freezing at -20°C overnight. Afterwards, all samples were freeze-dried at -55°C for 48 h using a Modulyo benchtop freeze dryer. Agrs 100 and Ch-Agrs blend specimens were converted into hydrogels after cooling to room temperature. A schematic diagram for the preparation process of the blend scaffolds can be seen in Figure 1. The produced 3D porous scaffolds were kept in a desiccator containing anhydrous silica gel to maintain zero % humidity. Table 1 summarises the compositions and codes of the prepared scaffolds.
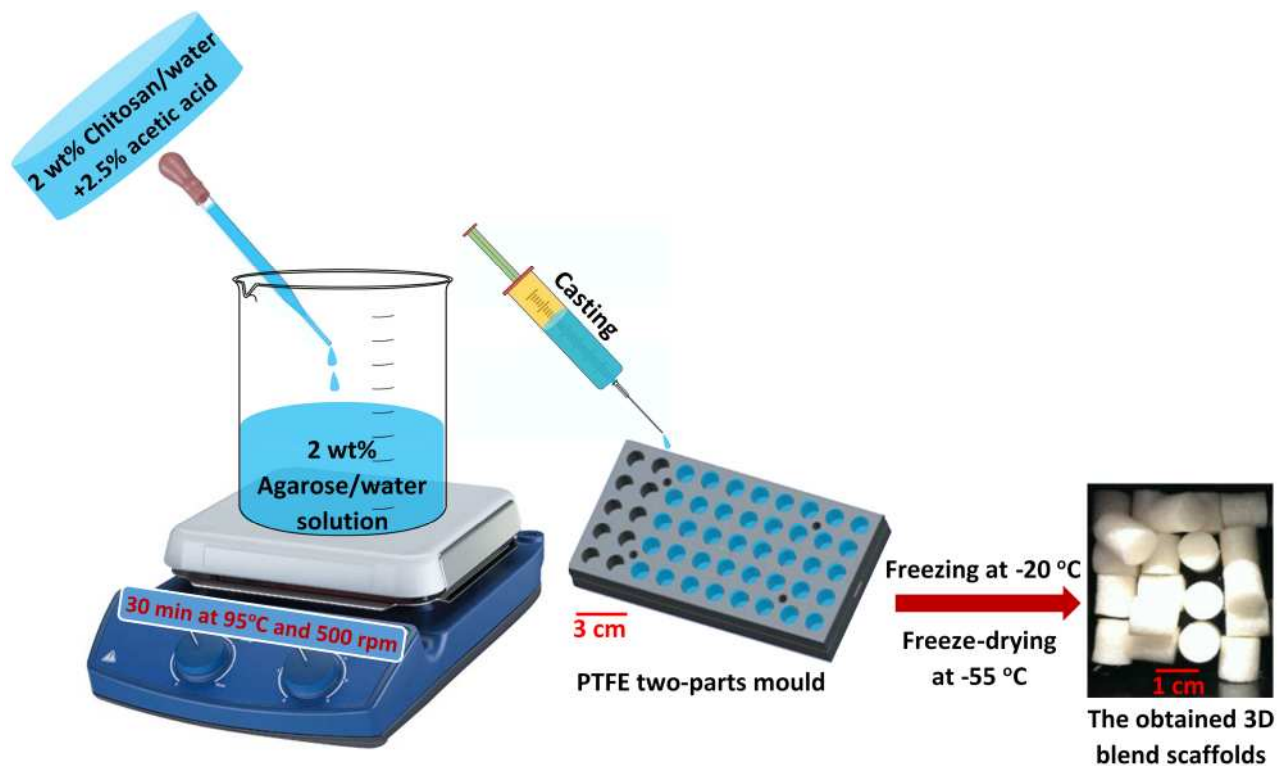
Figure 1: Schematic diagram for the preparation process of the Ch-Agrs blend scaffolds.

Table 1: Sample codes and compositions of various chitosan-agarose blend scaffolds.

Sample code used in this study	Chitosan solution (ml)	Agarose solution (ml)	Weight fractions in the blend	
			Chitosan (wt%)	Agarose (wt%)
Ch 100	20	0	100	0
Ch 75-Agrs 25	15	5	75	25
Ch 50-Agrs 50	10	10	50	50
Ch 25-Agrs 75	5	15	25	75
Agrs 100	0	20	0	100

2.3   Scanning electron microscope (SEM)

The microstructure and morphology of the Ch-Agrs blend scaffolds were examined using scanning electron microscopy (Philips XL 30) at a beam accelerated voltage of 10 kV, spot size of 4 and a working distance of 10 mm. The scaffolds were cut into 2 mm slices using a sharp blade, and sputter coated with platinum at 1.5 kV and 15 mA for 90 s. Pore sizes were determined from SEM micrographs using Image J 1.42 q software and at least 50 pores were chosen randomly from different micrographs. The mean pore sizes and standard errors were calculated and reported in this study.

2.4   Porosity of the scaffolds

An Archimedes method was used to determine the porosity of the scaffolds using ethanol as the liquid medium (Roohani-Esfahani, Newman, & Zreiqat, 2016). Low vacuum was applied using a 50ml plastic syringe to remove air from the scaffolds in order to fully submerge them in the ethanol. The porosity (φ) of the scaffold was determined in triplicate for each scaffold using the following equation:

$$\varphi = 1 - (\frac{\rho_{Bulk}}{\rho_{True}}) \times 100$$

where ρ_{bulk} and ρ_{True} are the bulk and true densities of the scaffold.

2.5   Thermal properties of the Ch-Agrs blend scaffolds

Thermal characteristics and thermogravimetric analysis of the scaffolds were carried out from 25°C to 600°C using a SDT Q600 analyser (TA instruments, USA) at a heating rate of 10 °C.min^{-1} and a nitrogen gas flow rate of 100 ml.min^{-1} on a 7 mg sample. A baseline for background correction was performed and triplicates were tested for each sample. The results were processed using TA Universal analysis 2000 software.

2.6   Fourier transform infrared spectroscopy (FTIR)

The functional groups of chitosan, agarose and their blend scaffolds were determined by FTIR spectroscopy in attenuated total reflectance (ATR) using Tensor-27 from Bruker. The samples were scanned in absorbance mode over the range of 4000 to 550 cm^{-1} wavenumber.

2.7   Swelling properties of the scaffolds

The swelling behaviour of the scaffolds was investigated by immersion in phosphate buffered saline (PBS) media at 37°C for 54 h. Changes in pH of the PBS and mass of the scaffolds were recorded at different time points. After removing samples from the PBS solution, they were systematically tapped 3 times to remove excess PBS before recording their weight (M_w) using a 5 digit balance. Swelling percentages of the scaffold were calculated using the following formula:

$$Swelling\ (\%) = \frac{(M_w - M_d)}{M_d}\ x\ 100$$

where M_d is the initial weight of the dry scaffold.

2.8   Compression testing

The compressive properties of the scaffolds were determined using a mechanical tester (Instron 5969 equipped with a 100 N load cell) at a compression rate of 1 mm.min^{-1} up to 50% strain. This

test was applied on both wet and dry samples in triplicate. The scaffolds were submerged in PBS for 24 h to reach saturation prior to testing as wet. The setup of the test and calculations of compressive strength and modulus were performed in accordance with British Standard ISO 844:2014. Compressive strength was determined as the compressive stress at 10% strain, while the modulus was calculated as the gradient of the initial linear portion in the stress-strain curve.

2.9 Statistical Analysis

One way analysis of variance (ANOVA) with Tukey's post-test was conducted on the results of the swelling and mechanical tests to determine the significance (P value) in the differences between the means using Graphpad Prism (Version 5.01) software.

3 Results and Discussion

3.1 Microstructure of the scaffolds

Cross sectional SEM micrographs of the prepared scaffolds are shown in Figure 2. Both unblended agarose and chitosan scaffolds showed larger pore sizes (mean *ca.* 550 µm), whilst the blend scaffolds demonstrated at least a factor 2 smaller (P<0.001) mean pore sizes, see Figure 3. The pore sizes of the blend scaffolds was reduced significantly from *ca.* 300 to 150 µm as the agarose content increased from 25 to 75 wt%. This could be attributed to the mechanism of the pores formation suggested by Chaudhary *et al.* (Chaudhary, Vadodariya, Nataraj, & Meena, 2015). They proposed that large pores were formed from chitosan chains and that the agarose chains were then trapped within them. Therefore, an increase of agarose content would lead to an increased quantity of trapped agarose chains thereby reducing the pore size.

Pre-gelation of Ch-Agrs blends before freezing due to the presence of the thermogelling agarose could be another reason for the reduction in their pore sizes. Hoffmann *et al.* (Hoffmann, Seitz, Mencke, Kokott, & Ziegler, 2009) reported that pre-gelation of chitosan via crosslinking using glutaraldehyde before freeze drying was influential on the pore size and geometry. The pore size was smaller compared to non-crosslinked chitosan which suggests an interaction between agarose and chitosan in the blends that has a similar effect to crosslinking. Similarly, the pore size for collagen scaffolds decreased from 100 - 200 µm to 50 - 150 µm by blending with 25 wt% of chitosan. This was attributed to the nature of chitosan as a semicrystalline polymer that tends to form membrane parts within the pores and lead to reduction in the pore size (Yan *et al.*, 2010). Moreover, the pore size of freeze- dried chitosan-polyvinyl alcohol (Ch-PVA) scaffolds was also investigated and it was found that the pore size of Ch 37.5-PVA 62.5 (wt%) was approximately 40% higher than Ch 16.7-PVA 83.3 scaffolds (Silva, Macedo, Coletta, Feldman, & Pereira, 2016).

The chitosan scaffold (Ch 100) reported here exhibited a different structure than that shown by the blends and pure agarose, having a layered lamella-like structure. Due to the lack of symmetry of the pores within all types of scaffolds, major and minor axes of individual pores were measured and the mean value was considered as the pore size. It was found that blending chitosan not only reduced the pore size, but also changed the pore geometry from elongated ellipsoid into nearly rounded pores. The elongated shape of the pores in Ch 100 led to the larger standard error of the mean. The elongated pores of chitosan scaffolds was also reported by Suh and Mathew (Francis Suh & Matthew, 2000).
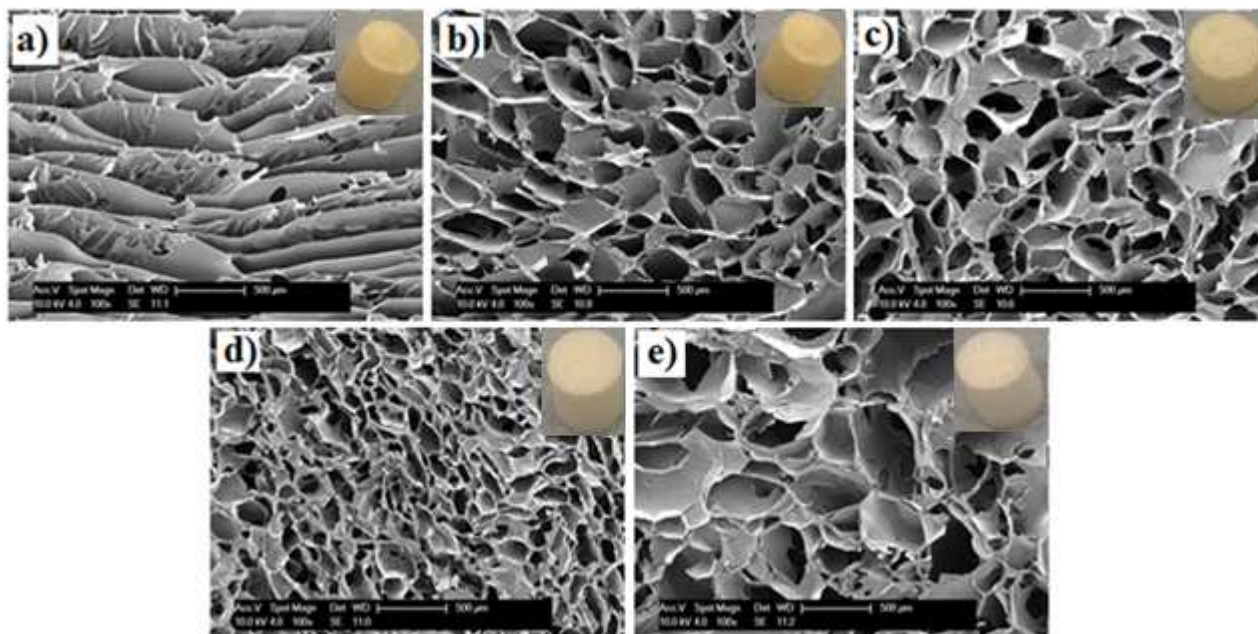
Figure 2: Cross-sectional SEM micrographs of chitosan-agarose blend (Ch-Agrs) scaffolds fabricated from different combinations of the two materials: (a) Ch 100, (b) Ch 75-Agrs 25, (c) Ch 50-Agrs 50, (d) Ch 25-Agrs75 and (e) Agrs 100. Scale bars = 500 µm. Photographs of the scaffolds are attached to the related SEM micrographs.
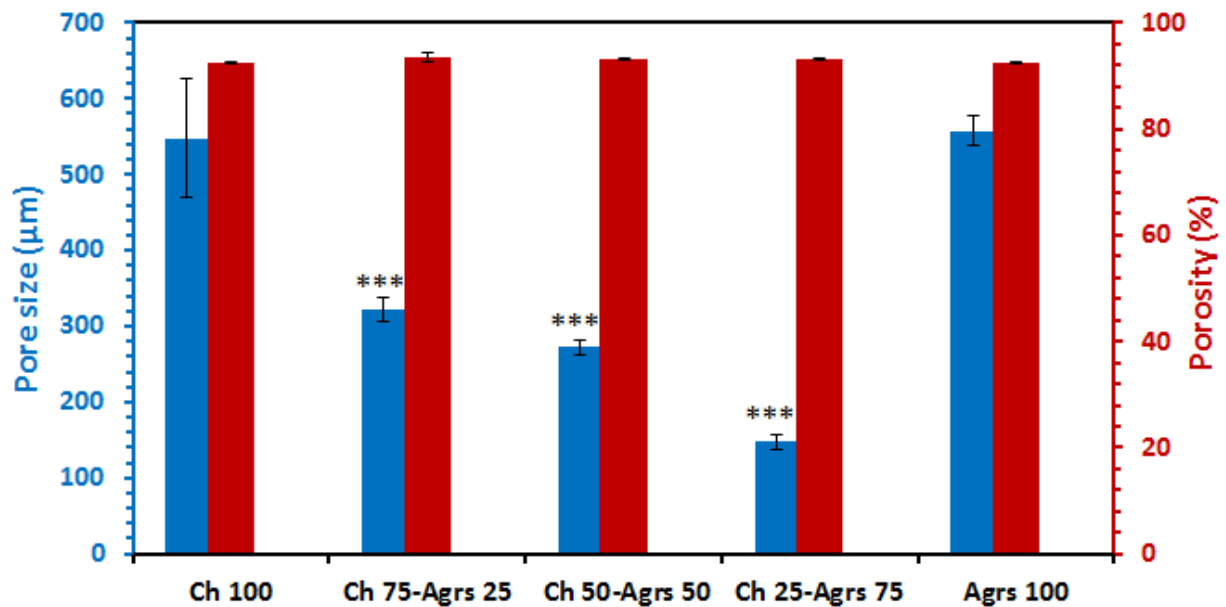
Figure 3: Average pore size and porosity of Ch-Agrs scaffolds. Dimensions (major and minor axes) of at least 50 pores were measured and the mean (±SEM) is represented. Porosity test was conducted in triplicate for each type of scaffold using Archimedes method. *** represent significant difference P<0.001.

The variety of pore sizes observed would potentially give rise to different applications. Larger pores are usually beneficial for cell attachment (Loh & Choong, 2013; Matsiko, Gleeson, & O'Brien, 2014), whilst smaller pores would improve mechanical performance of the porous construct (Berthod *et al.*, 1994; Cordell, Vogl, & Wagoner Johnson, 2009; Loh & Choong, 2013).

Figures 3 shows the percentage of porosity for Ch-Agrs blend scaffolds. Since a fixed polymer to solvent concentration was used in the preparation of all scaffolds, they show a similar porosity of 93 ± 1 % (P>0.05). This shows the consistency of the fabrication process of the scaffolds. This high level of porosity is favourable for biomedical purposes to enhance cell seeding, cell migration and delivery of cell nutrients and oxygen leading to tissue ingrowth (Hollister, 2005). However this high porosity would have adverse effects on the mechanical performance of the scaffolds (Lin, Kikuchi, & Hollister, 2004). Therefore, a balance between biological and mechanical properties of the scaffolds is always required in order to suit the end application of the implant, achievable by varying the polymer to solvent concentration.

3.2   Thermal properties of the scaffolds

The thermal properties of Ch-Agrs blend scaffolds were evaluated using DSC and TGA, see Figures 4a and 4b. Dehydration and decomposition are the thermal degradation mechanisms of polymers that can be explored using the TGA technique. A dehydration mechanism usually occurs at 100°C

due to the evaporation of residual moisture within the specimen, while decomposition happens at higher temperatures (i.e. decomposition temperature) and is commonly associated with carbonisation of the polymer and ash formation (Grohens, Thomas, & Jyotishkumar, 2015). All samples were dried overnight in an oven at 50°C to eliminate the residual moisture within the scaffold and kept in the oven prior to the thermal testing. No significant endothermic peaks or decreases in the weight were seen in the DSC and TGA thermographs at 100°C showing the effectiveness of the drying stage. If insufficient drying is applied then endothermic peaks and a 10-15% drop in the specimen weight is typically observed for Ch-Agrs blends (Trivedi, Rao, & Kumar, 2014).

The decomposition temperatures for the Ch-Agrs blend scaffolds (*ca.* 234 - 238°C) were significantly lower than for chitosan and agarose alone (*ca.* 280°C and 257°C respectively). The reduction in decomposition temperature for the blends could be attributed to the decrease in molecular weight of chitosan due to heating at 95°C for 15 min during preparation of the blend scaffolds. Jarry *et al.* (Jarry *et al.*, 2001) investigated the influence of steam sterilisation at 121 °C on molecular weight of chitosan based hydrogels and reported a 30% drop in the molecular weight after 10 min of sterilisation. The residual weight at the end of the TGA test for the blend scaffolds were higher than for chitosan or agarose alone, see Figure 4b. For example, Ch 50-Agrs 50 showed 5% and 10% increase in the residual mass compared to Ch 100 and Agrs 100 respectively. The increase in the residual mass of Ch-Agrs blends has been reported previously (Chaudhary, Vadodariya, Nataraj, & Meena, 2015) and attributed to an enhancement in the blend network as a result of hydrogen bonding between chitosan and agarose chains. This suggestion was confirmed by comparing the residual masses of non-crosslinked and genipin crosslinked Ch-Agrs blends that showed a 15 - 20% increase in final mass of the crosslinked blends, while the non-crosslinked blend showed a 5 - 10% increase in comparison with chitosan and agarose alone (Chaudhary, Vadodariya, Nataraj, & Meena, 2015). Therefore, a significant increase in the ash weight of the blend was obtained due to covalent bonding between chitosan and agarose via the genipin-based crosslinks.

The DSC and TGA findings revealed that the blend scaffolds reported here are thermally stable up to *ca.* 180°C suggesting that they can be sterilised using the autoclave method at 121°C, which is more cost-effective and less destructive than gamma ray sterilisation for polymers (Tripathi & Melo, 2015).
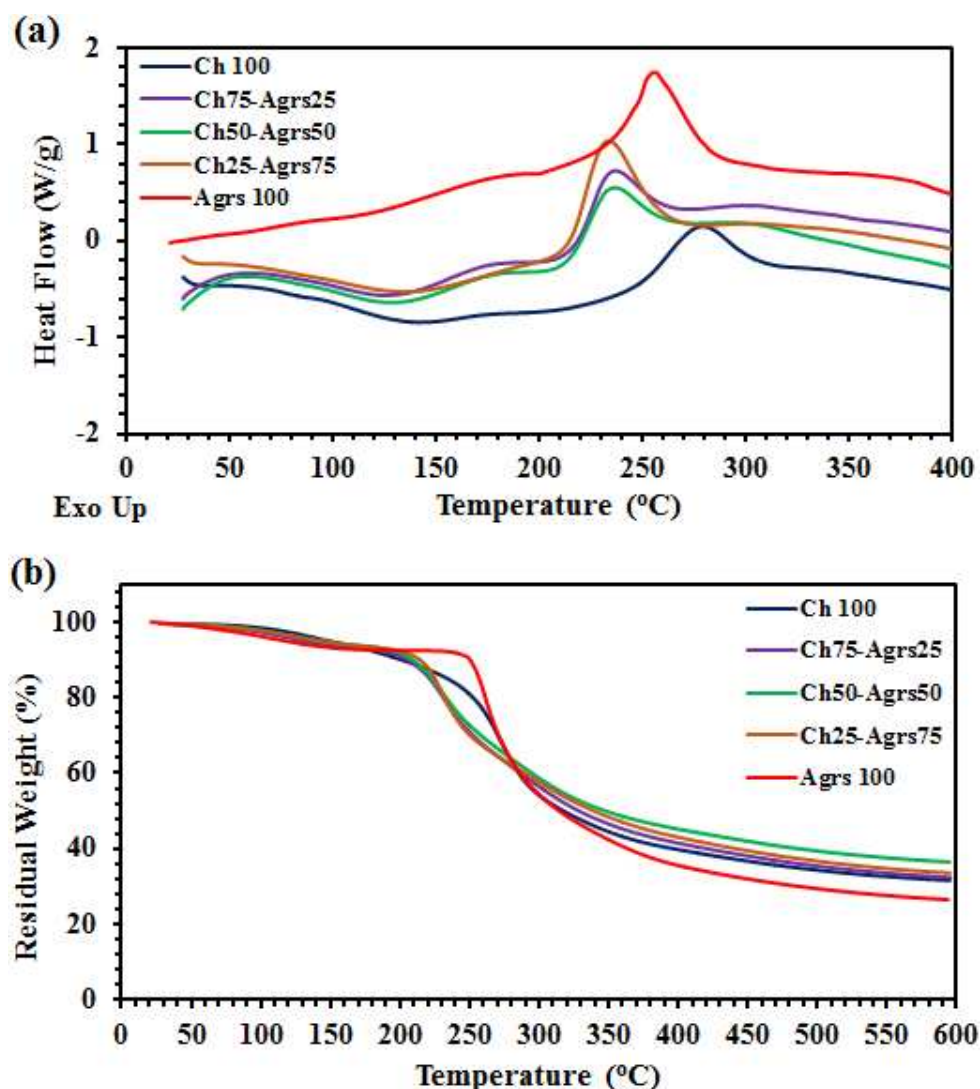
Figure 4: Thermal properties of chitosan, agarose and Ch-Agrs blend scaffolds: (a) DSC traces and (b) TGA thermographs. Both DSC and TGA testes were carried out at heating rate of 10 °C min^{-1} under nitrogen gas.

3.3 Fourier transform infrared spectroscopy (FTIR)

The functional groups of chitosan, agarose and their various blends were studied using FTIR analysis as shown in Figure 5a. Chitosan exhibited a characteristic broad band around 3100-3550 cm^{-1} with highest peak at 3260 cm^{-1} which was attributed to -NH$_2$ and –OH stretching vibrations; agarose also showed a similar broad spectrum peak at 3363 cm^{-1} due to O-H stretching vibrations. However, in the case of the various blends of Ch-Agrs the associated peaks for -NH$_2$ and -OH stretching vibrations were seen to shift to higher frequencies (for example, from 3260 cm^{-1} towards 3363 cm^{-1}), which can be attributed to the formation of hydrogen bonds between the -NH$_2$/-OH groups of chitosan and the -OH groups of agarose (Trivedi, Rao, & Kumar, 2014) as depicted in Figure 5b. Chitosan and its blends also showed an absorbance band at 1560 cm^{-1} which is associated with NH bending and the intensity of this band decreased as the chitosan content decreased in the Ch-Agrs blends. Peaks

11

observed at 2923, 1560, 1409 cm^{-1} are assigned to the CH$_2$ bending (pyranose ring); that at 1635 cm^{-1} to the C=O stretching vibration; peaks at 1069 and 1027 cm^{-1} to the saccharide structure, and the band at 647 cm^{-1} to the =C-H bond bending (Trivedi, Rao, & Kumar, 2014). On the other hand, pure agarose and its blends also showed the presence of all the characteristic absorbance bands of agarose at 931 cm^{-1} (due to 3,6-anhydrogalactose bending), 1151 and 1040 cm^{-1} (C—O stretching vibration) (Chaudhary, Vadodariya, Nataraj, & Meena, 2015).
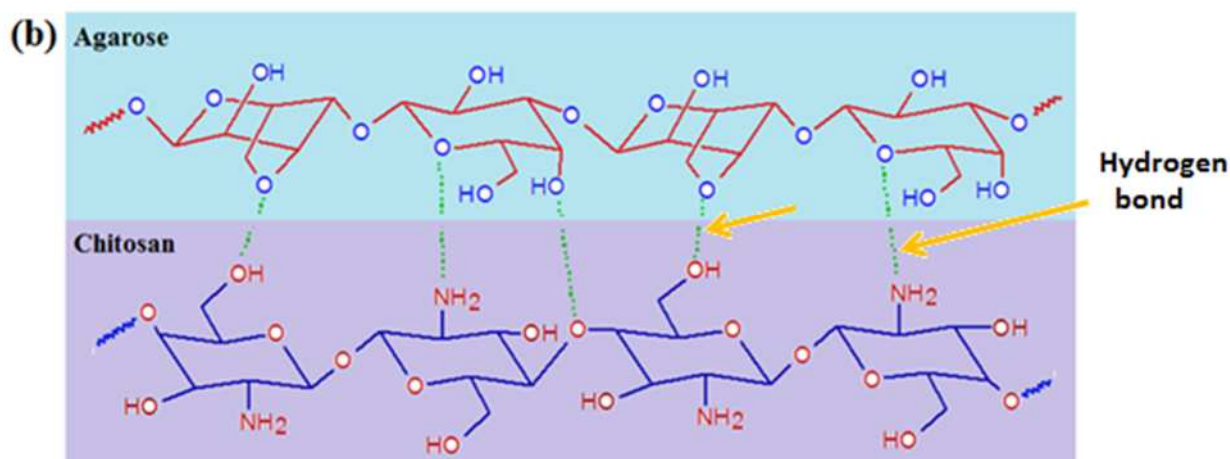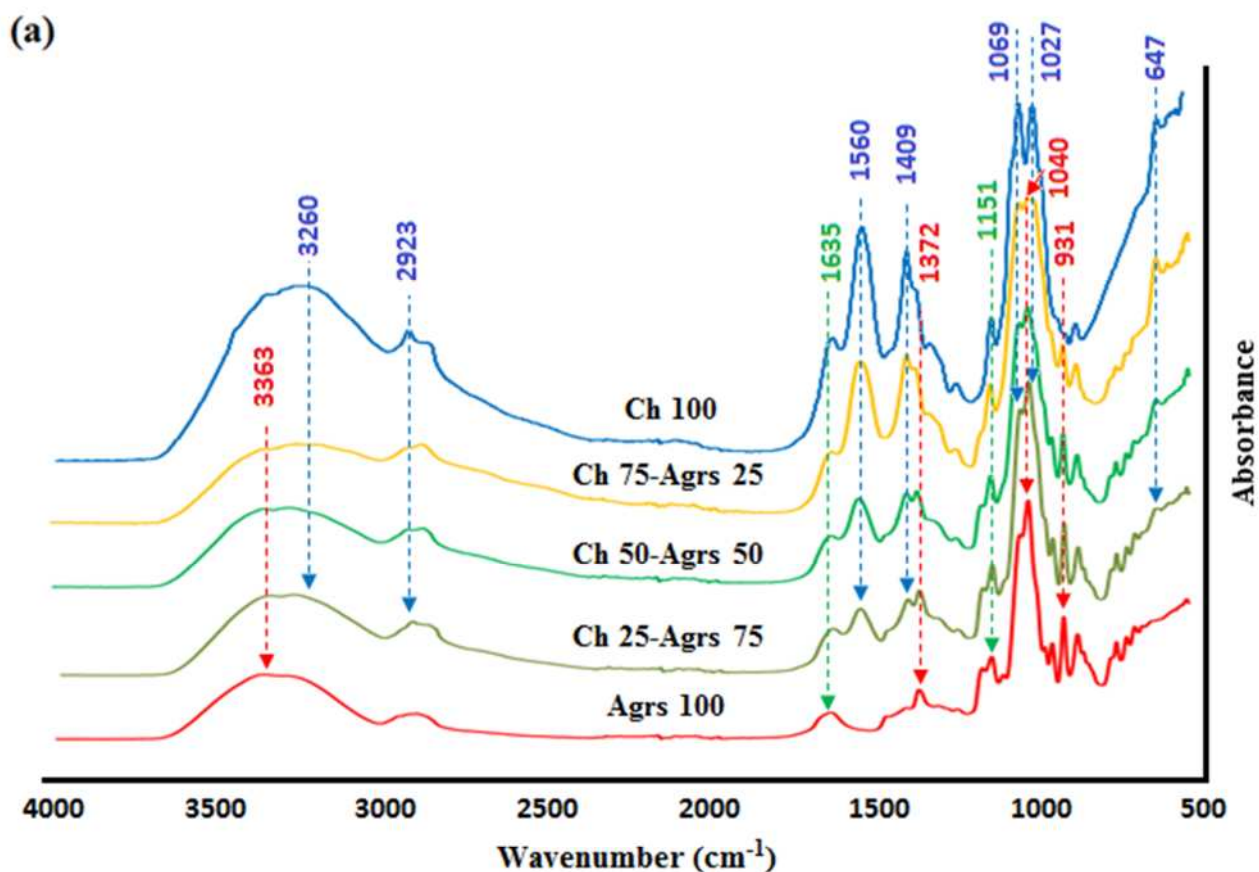

Figure 5: Structural analysis of Ch-Agrs blend scaffolds: (a) FTIR spectra and (b) schematic diagram for the expected chemical interaction between chitosan and agarose with the blend scaffolds where the green dot lines represent the hydrogen bonding.

3.4   Swelling profiles of Ch-Agrs blend scaffolds in PBS

Swelling of scaffolds in aqueous media can be sometimes desirable in biomedical applications because the pore size would increase initially and accommodate cells, although swelling of the scaffold would lead to weaker mechanical properties (Li, Ramay, Hauch, Xiao, & Zhang, 2005). The percentage swelling is highly dependent on the pH of the aqueous media (H.-S. Lee *et al.*, 2012; O.-S. Lee, Ha, Park, & Lee, 1997). Since the target application of these scaffolds is biomedical, the swelling behaviour of Ch-Agrs scaffolds was assessed in PBS (pH ~7.4), see Figure 6a. All scaffolds absorbed large quantities of PBS, ranging from 800 to 1200% after 15 min, followed by a gradual increase at a rate of 0.75 – 1.25 % per min to reach saturation levels after 6 h. The high swelling tendency of these scaffolds could be attributed to the hydrophilicity nature of both chitosan and agarose (Alonso Gabriel, Rivera José Luis, Mendoza Ana María, & Mendez Maria Leonor, 2007) and the presence of hydroxyl and amino (-OH and $-NH_2$) functional groups (Hu *et al.*, 2016). The inset bar chart (Figure 6a) shows the percentage of scaffold swelling after saturation. The Ch 100 and Ch 75-Agrs 25 scaffolds demonstrated the highest swelling ratio (*ca.* 1500%), and Ch 50-Agrs 50 scaffolds the lowest (P<0.001) blend scaffolds showing similar swelling as the plain agarose scaffold, suggesting that the 50-50 composition is near to the optimum interaction between chitosan and agarose. This finding correlates well with the residual weight results from TGA test as the Ch 50-Agrs 50 scaffolds showed the highest final mass at 600 ºC.

The Ch 100 scaffolds were unstable in PBS and fully disintegrated after 24 h, at which point it became impossible to continue taking measurements for it (Figure 6b). The other scaffolds remained intact until the end of the swelling experiment, showing the stabilising effect of agarose incorporation. After 6 h of immersion in PBS, all scaffolds were stable at *ca.* 1300 -1500% uptake until the end of the experiment (Figure 6a). The high capacity of these blend scaffolds for water uptake could be ascribed to the existence of hydrophilic functional groups such as carboxyl, amino and hydroxyl as detected from FTIR spectra (Hu *et al.*, 2016), Figure 5a.
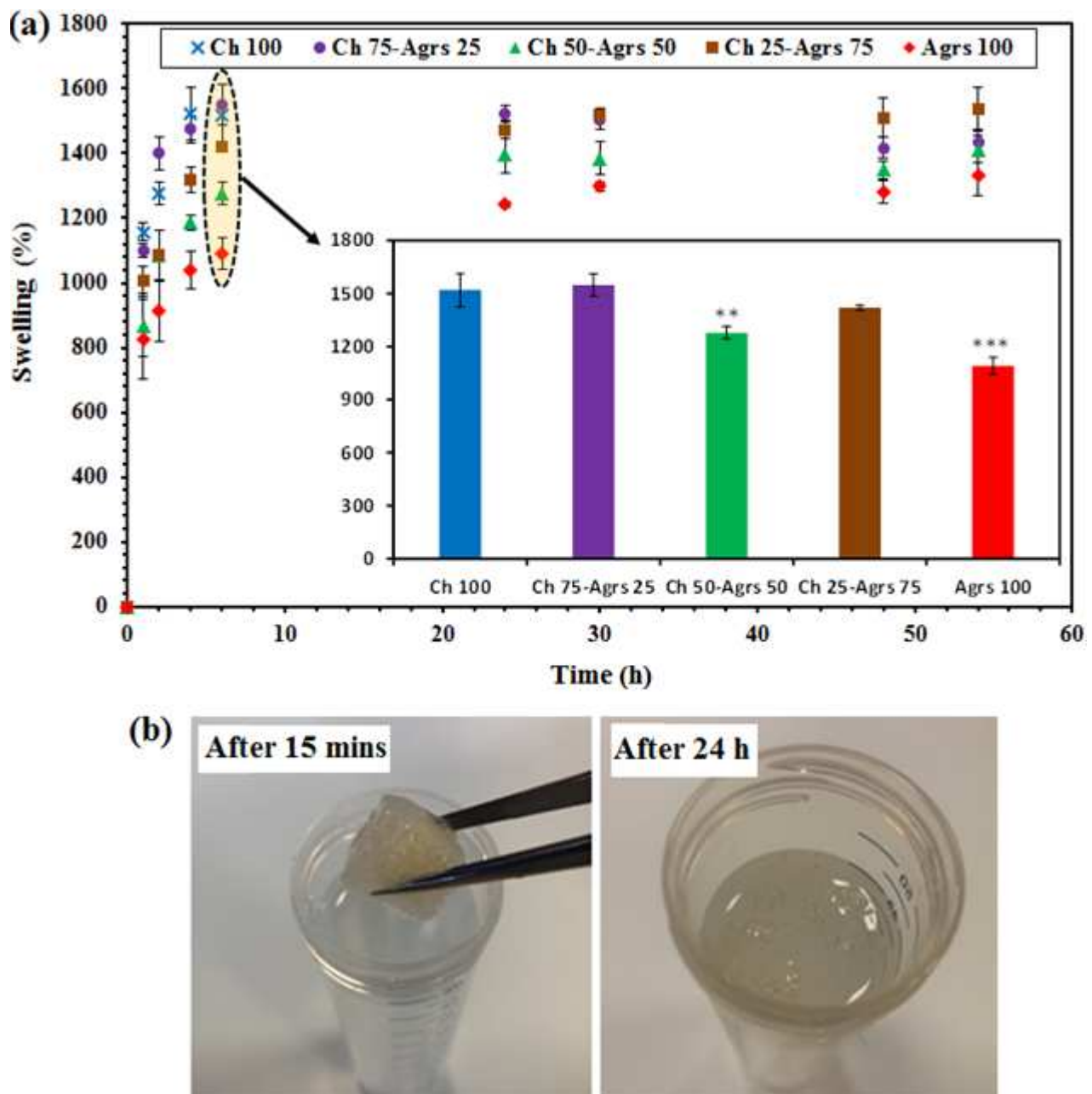
Figure 6: Swelling profiles of Ch-Agrs scaffolds in PBS at 37°C: (a) swelling percentage of the scaffolds versus time and (b) optical photographs of Ch 100 scaffolds after 15 min and 24 h showing that pure chitosan scaffolds are fully disintegrated after 6 h soaking in PBS. Inset bar chart represents swelling percentages for all scaffolds after saturation (6 h). Triplicates (n=3) of each type of scaffolds were measured and swelling percentage was calculated ±SD. ** and *** represent significant difference P<0.01 and P<0.001 respectively.

3.5 Compressive properties of Ch-Agrs scaffolds

Compression tests were applied on dry and wet scaffolds up to 50% strain. Stress-strain curves for the dry samples can be seen in Figure 7. All scaffolds revealed a typical compressive stress-strain profile of porous polymeric materials (Gil *et al.*, 2011). The scaffolds exhibited three regions; initial linear elastic region to 5 - 10 % strain, then a plateau region up until around 50% strain and finally

a densification region beyond that due to the gradual compressing of the pores (Gil *et al.*, 2011). The densification region cannot be observed in Figure 7 as the test was stopped at 50% strain.
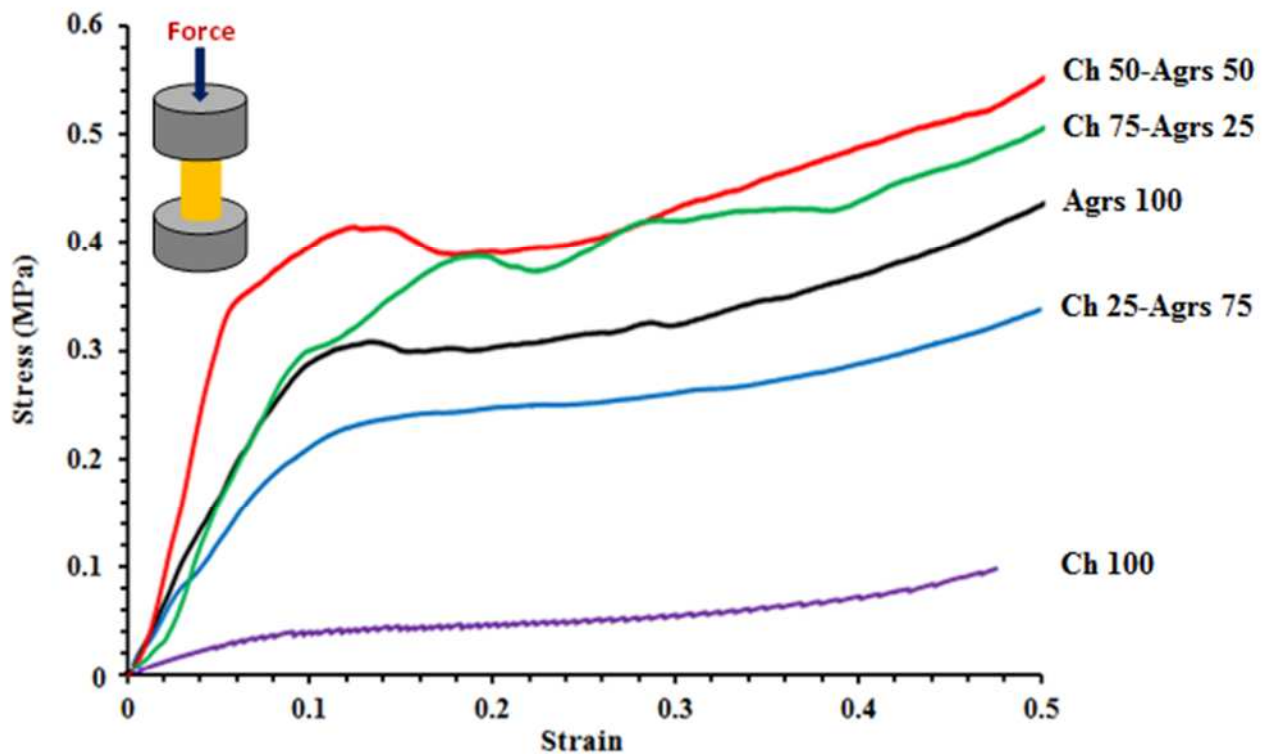

Figure 7: Representative compressive stress-strain curves for Ch 100, Agrs 100 and their blend scaffolds tested dry at room temperature. A schematic diagram of the compression test setup can be seen in the inset figure.

Bar charts for the compressive properties of Ch-Agrs blend scaffolds tested dry and wet can be seen in Figure 8. For dry scaffolds, Ch 100 showed the lowest properties (P<0.001) (*ca.* 0.24 and 0.02 MPa for modulus and strength) compared to other compositions, Figure 8a. Compressive properties of Agrs 100 were 10 times higher (P<0.001) than Ch 100. Therefore, significant increases (P<0.001) in both the strength and modulus were obtained by incorporation of agarose as expected. For instance, Ch 75-Agrs 25 blend scaffolds had compressive modulus and strength of approximately 3.1 and 0.28 MPa (around 13 times higher than Ch 100) respectively. The CH 50-Agrs50 blend scaffold revealed the highest (P<0.001) compressive modulus and strength values (4.5 ± 0.4 and 0.35 ± 0.03 MPa respectively) while a further increase in the amount of agarose (75 wt%) was found to decrease the compressive modulus and strength to 2 MPa and 0.28 MPa respectively. The increase in mechanical properties of Ch 75-Agrs 25 and Ch 50-Agrs 50 scaffolds in comparison with Ch 100 and Agrs 100 could also be attributed to the decrease in the pore size (Cordell, Vogl, & Wagoner Johnson, 2009; Klotz, Gawlitta, Rosenberg, Malda, & Melchels, 2016), see Figure 3.

The mechanical properties of polymer blends usually give an indication of possible interaction between the constituents (Kar, Biswas, & Bose, 2015). The significant increase in compressive strength and modulus for Ch 50-Agrs 50 and Ch 75-Agrs 25 blends under dry conditions indicated a possible reaction between chitosan and agarose within the blend via hydrogen bonding as suggested above and also reported in the literature (Chaudhary, Vadodariya, Nataraj, & Meena, 2015; Hu *et al.*, 2016; Trivedi, Rao, & Kumar, 2014). The improved mechanical properties of chitosan are often related to a crosslinking process (Hoffmann, Seitz, Mencke, Kokott, & Ziegler, 2009). Therefore it is postulated that agarose is acting as a crosslinker here.

After saturation of the scaffolds in PBS for 24 h at 37°C, the Ch 100 scaffolds disintegrated and mechanical testing was not possible, see Figure 6b. A significant decrease can be seen in the compressive properties of all scaffolds due to the water adsorption, Figure 8b. The wet Agrs 100 scaffold had the greatest modulus and strength (P<0.001) of approximately 0.13 MPa. Compressive properties of wet blend scaffolds was *ca.* 50% lower than Agrs 100 which might be ascribed to the higher capability of chitosan to adsorb water compared to agarose, see Figure 6a. Under wet conditions, the plasticisation effect of water would dominate the compressive properties of the scaffolds (Felfel *et al.*, 2012). The weakening of the hydrogen bonding between chitosan and agarose in aqueous media is another possible reason for this reduction in the mechanical properties of the blend scaffolds by a factor of two compared to agarose alone.
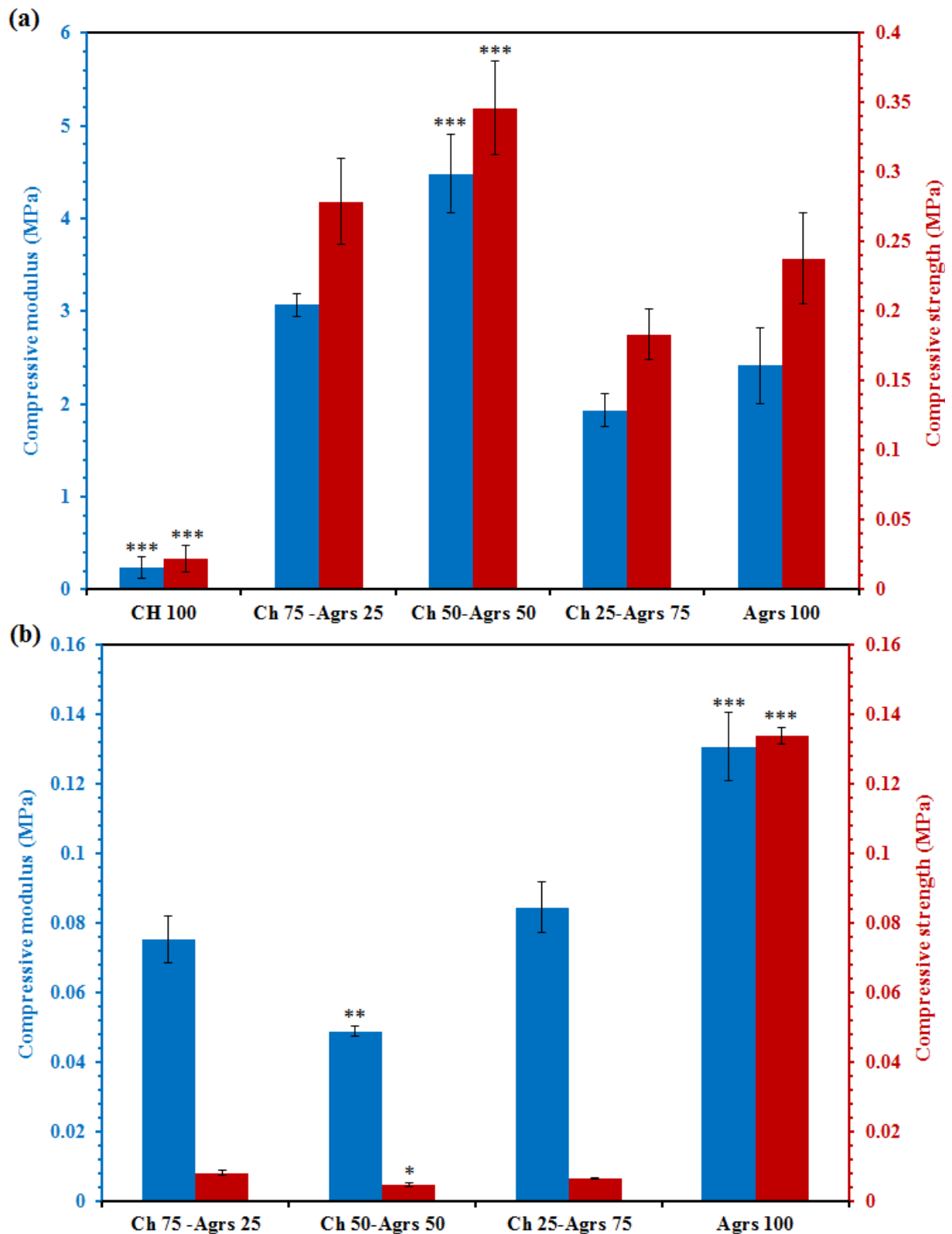
*Figure 8: Compressive properties of Ch-Agrs scaffolds: (a) tested dry and (b) tested wet after submersion in PBS for 24 h. Triplicates (n=3) of each specimens were tested and compressive strength and modulus were determined according to the standard method. Error bars represent standard deviation. No data is presented for the wet Ch 100 scaffold because it was fully disintegrated after soaking in PBS for 24 h. *, ** and *** represent significant difference P<0.05, P<0.01 and P<0.001 respectively.*

Cancellous bone has a range of mechanical properties with a compressive modulus of 0.1 – 0.5 GPa and compressive strength of 4 - 12 MPa (Liu, 2016) and there is still an order of magnitude between these values and those of the scaffolds, but scaffolds used in this way only need to retain their integrity long enough for cells to grow and new tissue to form (O'Brien, 2011). However, these scaffolds would be more suited to cartilage repair, soft tissue engineering or low load-bearing hard tissue grafting. Furthermore, the mechanical properties of these scaffolds can be enhanced by inclusion of nanoparticles such as hydroxyapatite which would be beneficial for bone grafting (Thein-Han & Misra, 2009), or silver nanoparticles for wound dressings (You *et al.*, 2017). For example when 0.7 % (wt/wt) of tricalcium phosphate particles (0.85 μm of average diameter) were added to chitosan-gelatine blend scaffolds, their compressive modulus and strength increased from 3.9 ± 1 and 0.29 ± 0.02 MPa to 10.9 ± 3.5 and 0.88 ± 0.05 MPa respectively (Yin *et al.*, 2003).

A blend of chitosan-alginate (50-50) scaffold with very similar porosity at 92% had a higher compressive modulus and strength (8.16 and 0.46 MPa respectively) (Li, Ramay, Hauch, Xiao, & Zhang, 2005) compared to the Ch 50-Agrs 50 composition presented here. This could be due to their crosslinking of the chitosan-alginate scaffolds using calcium chloride. When agarose was mixed with bacterial cellulose, the scaffolds produced had two orders of magnitude lower modulus at 55 kPa and order of magnitude lower strength 43 kPa strength (Yang *et al.*, 2011) which might be due to the lack of reaction between agarose and cellulose.

When the scaffolds are compressed dry, they are plastically deformed as expected. However, the hydrated scaffolds demonstrated fully reversible recovery see (Figure 9). The Ch-Agrs blend scaffolds showed instant recovery after full compression as wet. This extensive recovery property would facilitate the injectability of the porous constructs as the implant could be fully compressed without damage during the injection process and then could return to the original shape and function at the desired site in the human body (Montgomery *et al.*, 2017). This full recovery property would also be desirable for tissue patch applications such as cardiac patches (Bencherif *et al.*, 2012).
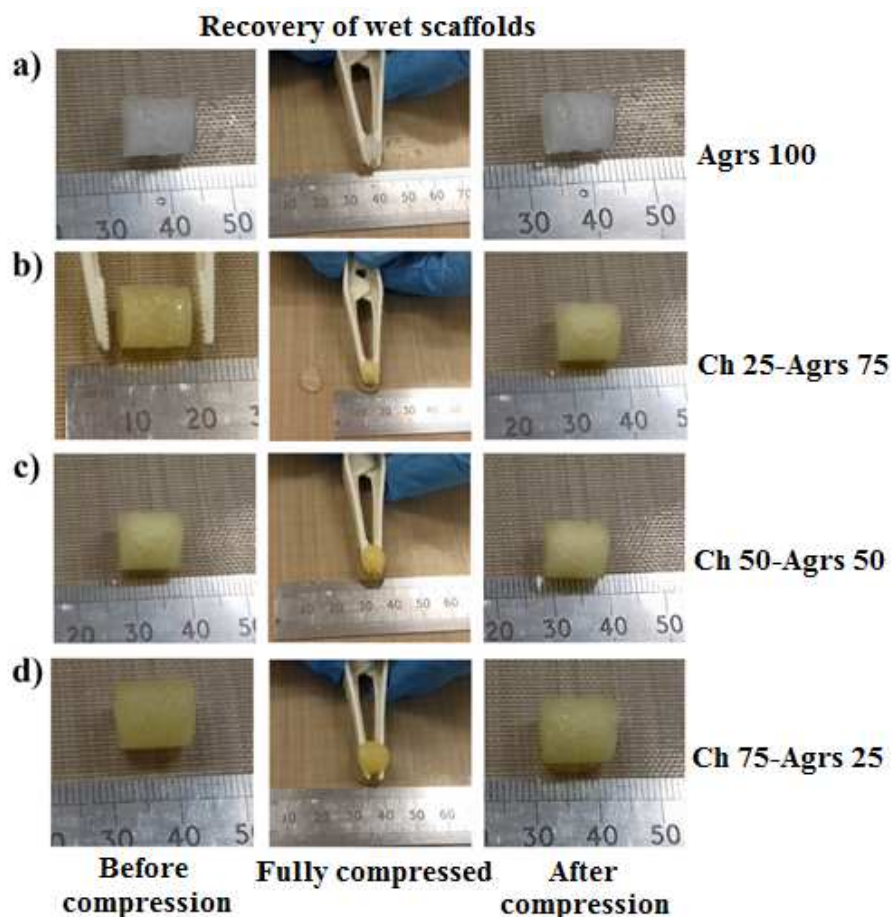
Figure 9: Photographs show the recovery profiles of Ch-Agrs blend scaffolds. All compositions exhibited instantaneous recovery after full compression using plastic tweezers. A Ch100 scaffold is not included in this experiment due its lack of stability in aqueous media.

Thus, blending agarose with chitosan was found to be beneficial. Significant enhancement in swelling and compressive properties were obtained for Ch 50-Agrs 50 blend scaffolds, suggesting a hydrogen bonding reaction between chitosan and agarose. Their full recovery after compressing to less than 20% of its original volume offers practical advantages for the blend scaffolds in respect of their method of application. Consequently, these blend scaffolds could potentially be useful for soft tissue repair subject to more comprehensive in vitro and in vivo studies.

4   Conclusions

Highly porous structures were produced from chitosan, agarose and their blends. Increasing the agarose content in the blend led to significant reduction in pore size and significant increase in the compressive properties in comparison with both agarose and chitosan alone. The 100% chitosan scaffold was fully disintegrated in PBS after 24 h, however incorporation of agarose led to a significant improvement in the stability in aqueous media. After saturation in PBS, all blend scaffolds showed instant total recovery after full compression, which would ease the delivery of the scaffolds

into the defect during implantation. Enhancement in the mechanical and swelling performances of the blend scaffolds suggest a possible interaction between agarose and chitosan via hydrogen bonding. The scaffolds fabricated in this study show the potential for use in biomedical applications such as soft tissues repair.

5 Acknowledgements

6 References

A. Sionkowska, K. Lewandowska, A. Planecka, P. Szarszewska, K. Krasinska, B. Kaczmarek, & Kozlowska, J. (2014). Biopolymer Blends as Potential Biomaterials and Cosmetic Materials. *Key Engineering Materials,* 583.

Alonso Gabriel, J., Rivera José Luis, A., Mendoza Ana María, M., & Mendez Maria Leonor, H. (2007). Effect of temperature and pH on swelling behavior of hydroxyethyl cellullose-acrylamide hydrogel. *e-Polymers* (Vol. 7).

Amir Afshar, H., & Ghaee, A. (2016). Preparation of aminated chitosan/alginate scaffold containing halloysite nanotubes with improved cell attachment. *Carbohydrate Polymers,* 151(Supplement C), 1120-1131.

Bencherif, S. A., Sands, R. W., Bhatta, D., Arany, P., Verbeke, C. S., Edwards, D. A., & Mooney, D. J. (2012). Injectable preformed scaffolds with shape-memory properties. *Proc Natl Acad Sci U S A,* 109(48), 19590-19595.

Berthod, F., Saintigny, G., Chretien, F., Hayek, D., Collombel, C., & Damour, O. (1994). Optimization of thickness, pore size and mechanical properties of a biomaterial designed for deep burn coverage. *Clinical Materials,* 15(4), 259-265.

Bhat, S., & Kumar, A. (2012). Cell proliferation on three-dimensional chitosan–agarose–gelatin cryogel scaffolds for tissue engineering applications. *Journal of Bioscience and Bioengineering,* 114(6), 663-670.

Bhat, S., Tripathi, A., & Kumar, A. (2010). Supermacroprous chitosan–agarose–gelatin cryogels: in vitro characterization and in vivo assessment for cartilage tissue engineering. *Journal of The Royal Society Interface.*

Cao, Z., Gilbert, R. J., & He, W. (2009). Simple Agarose−Chitosan Gel Composite System for Enhanced Neuronal Growth in Three Dimensions. *Biomacromolecules,* 10(10), 2954-2959.

Chaudhary, J. P., Vadodariya, N., Nataraj, S. K., & Meena, R. (2015). Chitosan-Based Aerogel Membrane for Robust Oil-in-Water Emulsion Separation. *ACS Applied Materials & Interfaces,* 7(44), 24957-24962.

Cordell, J. M., Vogl, M. L., & Wagoner Johnson, A. J. (2009). The influence of micropore size on the mechanical properties of bulk hydroxyapatite and hydroxyapatite scaffolds. *Journal of the Mechanical Behavior of Biomedical Materials,* 2(5), 560-570.

Doulabi, A., Mequanint, K., & Mohammadi, H. (2014). Blends and Nanocomposite Biomaterials for Articular Cartilage Tissue Engineering. *Materials,* 7(7), 5327.

El-hefian, E. A., Nasef, M. M., & Yahaya, A. H. (2012). Preparation and Characterization of Chitosan/Agar Blended Films: Part 1. Chemical Structure and Morphology. *E-Journal of Chemistry,* 9(3).

Elieh-Ali-Komi, D., & Hamblin, M. R. (2016). Chitin and Chitosan: Production and Application of Versatile Biomedical Nanomaterials. *International Journal of Advanced Research,* 4(3), 411-427.

Felfel, R. M., Ahmed, I., Parsons, A. J., Haque, P., Walker, G. S., & Rudd, C. D. (2012). Investigation of Crystallinity, Molecular Weight Change, and Mechanical Properties of PLA/PBG Bioresorbable Composites as Bone Fracture Fixation Plates. *Journal of Biomaterials Applications,* 26(7), 765-789.

Francis Suh, J. K., & Matthew, H. W. T. (2000). Application of chitosan-based polysaccharide biomaterials in cartilage tissue engineering: a review. *Biomaterials,* 21(24), 2589-2598.

Gil, E. S., Kluge, J. A., Rockwood, D. N., Rajkhowa, R., Wang, L., Wang, X., & Kaplan, D. L. (2011). Mechanical Improvements to Reinforced Porous Silk Scaffolds. *Journal of Biomedical Materials Research. Part a,* 99(1), 16-28.

Grohens, Y., Thomas, S., & Jyotishkumar, P. (2015). *Characterization of Polymer Blends: Miscibility, Morphology and Interfaces*: Wiley-VCH.

Haugh, M. G., Murphy, C. M., & O'Brien, F. J. (2009). Novel Freeze-Drying Methods to Produce a Range of Collagen–Glycosaminoglycan Scaffolds with Tailored Mean Pore Sizes. *Tissue Engineering Part C: Methods,* 16(5), 887-894.

Hoffmann, B., Seitz, D., Mencke, A., Kokott, A., & Ziegler, G. (2009). Glutaraldehyde and oxidised dextran as crosslinker reagents for chitosan-based scaffolds for cartilage tissue engineering. *Journal of Materials Science: Materials in Medicine,* 20(7), 1495-1503.

Hollister, S. J. (2005). Porous scaffold design for tissue engineering. *Nature Materials,* 4, 518.

Hu, Z., Hong, P., Liao, M., Kong, S., Huang, N., Ou, C., & Li, S. (2016). Preparation and Characterization of Chitosan—Agarose Composite Films. *Materials,* 9(10), 816.

Jarry, C., Chaput, C., Chenite, A., Renaud, M. A., Buschmann, M., & Leroux, J. C. (2001). Effects of steam sterilization on thermogelling chitosan-based gels. *Journal of Biomedical Materials Research,* 58(1), 127-135.

Jayakumar, R., Menon, D., Manzoor, K., Nair, S. V., & Tamura, H. (2010). Biomedical applications of chitin and chitosan based nanomaterials—A short review. *Carbohydrate Polymers,* 82(2), 227-232.

Kar, G. P., Biswas, S., & Bose, S. (2015). Simultaneous enhancement in mechanical strength, electrical conductivity, and electromagnetic shielding properties in PVDF-ABS blends

containing PMMA wrapped multiwall carbon nanotubes. *Physical Chemistry Chemical Physics,* 17(22), 14856-14865.

Klotz, B. J., Gawlitta, D., Rosenberg, A. J. W. P., Malda, J., & Melchels, F. P. W. (2016). Gelatin-Methacryloyl Hydrogels: Towards Biofabrication-Based Tissue Repair. *Trends in Biotechnology,* 34(5), 394-407.

Lee, H.-S., Yee, M. Q., Eckmann, Y. Y., Hickok, N. J., Eckmann, D. M., & Composto, R. J. (2012). Reversible swelling of chitosan and quaternary ammonium modified chitosan brush layers: effects of pH and counter anion size and functionality. *Journal of Materials Chemistry,* 22(37), 19605-19616.

Lee, O.-S., Ha, B.-J., Park, S.-N., & Lee, Y.-S. (1997). Studies on the pH-dependent swelling properties and morphologies of chitosan/calcium-alginate complexed beads. *Macromolecular Chemistry and Physics,* 198(9), 2971-2976.

Lewandowska, K., Sionkowska, A., & Grabska, S. (2015). Chitosan blends containing hyaluronic acid and collagen. Compatibility behaviour. *Journal of Molecular Liquids,* 212(Supplement C), 879-884.

Li, Z., Ramay, H. R., Hauch, K. D., Xiao, D., & Zhang, M. (2005). Chitosan–alginate hybrid scaffolds for bone tissue engineering. *Biomaterials,* 26(18), 3919-3928.

Lin, C. Y., Kikuchi, N., & Hollister, S. J. (2004). A novel method for biomaterial scaffold internal architecture design to match bone elastic properties with desired porosity. *Journal of Biomechanics,* 37(5), 623-636.

Liu, H. (2016). *Nanocomposites for Musculoskeletal Tissue Regeneration*: Elsevier Science.

Loh, Q. L., & Choong, C. (2013). Three-Dimensional Scaffolds for Tissue Engineering Applications: Role of Porosity and Pore Size. *Tissue Engineering Part B: Reviews,* 19(6), 485-502.

Mano, J. F., Silva, G. A., Azevedo, H. S., Malafaya, P. B., Sousa, R. A., Silva, S. S., . . . Reis, R. L. (2007). Natural origin biodegradable systems in tissue engineering and regenerative medicine: present status and some moving trends. *Journal of The Royal Society Interface,* 4(17), 999-1030.

Matsiko, A., Gleeson, J. P., & O'Brien, F. J. (2014). Scaffold Mean Pore Size Influences Mesenchymal Stem Cell Chondrogenic Differentiation and Matrix Deposition. *Tissue Engineering Part A,* 21(3-4), 486-497.

Merlin Rajesh Lal, L. P., Suraishkumar, G. K., & Nair, P. D. (2017). Chitosan-agarose scaffolds supports chondrogenesis of Human Wharton's Jelly mesenchymal stem cells. *J Biomed Mater Res A,* 105(7), 1845-1855.

Montgomery, M., Ahadian, S., Davenport Huyer, L., Lo Rito, M., Civitarese, R. A., Vanderlaan, R. D., . . . Radisic, M. (2017). Flexible shape-memory scaffold for minimally invasive delivery of functional tissues. *Nature Materials,* 16, 1038.

O'Brien, F. J. (2011). Biomaterials & scaffolds for tissue engineering. *Materials Today,* 14(3), 88-95.

Ragetly, G. R., Slavik, G. J., Cunningham, B. T., Schaeffer, D. J., & Griffon, D. J. (2010). Cartilage tissue engineering on fibrous chitosan scaffolds produced by a replica molding technique. *Journal of Biomedical Materials Research Part A,* 93A(1), 46-55.

Roohani-Esfahani, S.-I., Newman, P., & Zreiqat, H. (2016). Design and Fabrication of 3D printed Scaffolds with a Mechanical Strength Comparable to Cortical Bone to Repair Large Bone Defects. *Scientific Reports,* 6, 19468.

Sachlos, E., & Czernuszka, J. T. (2003). Making tissue engineering scaffolds work. Review: the application of solid freeform fabrication technology to the production of tissue engineering scaffolds. *Eur Cell Mater,* 5, 29-39; discussion 39-40.

Sarasam, A., & Madihally, S. V. (2005). Characterization of chitosan–polycaprolactone blends for tissue engineering applications. *Biomaterials,* 26(27), 5500-5508.

Shanmugasundaram, N., Ravichandran, P., Neelakanta Reddy, P., Ramamurty, N., Pal, S., & Panduranga Rao, K. (2001). Collagen–chitosan polymeric scaffolds for the in vitro culture of human epidermoid carcinoma cells. *Biomaterials,* 22(14), 1943-1951.

Silva, A. R. P. d., Macedo, T. L., Coletta, D. J., Feldman, S., & Pereira, M. d. M. (2016). Synthesis, characterization and cytotoxicity of Chitosan/Polyvinyl Alcohol/Bioactive Glass hybrid scaffolds obtained by lyophilization. *Matéria (Rio de Janeiro),* 21, 964-973.

Sionkowska, A. (2011). Current research on the blends of natural and synthetic polymers as new biomaterials: Review. *Progress in Polymer Science,* 36(9), 1254-1276.

Sionkowska, A., Wisniewski, M., Skopinska, J., Kennedy, C. J., & Wess, T. J. (2004). Molecular interactions in collagen and chitosan blends. *Biomaterials,* 25(5), 795-801.

Stokols, S., & Tuszynski, M. H. (2006). Freeze-dried agarose scaffolds with uniaxial channels stimulate and guide linear axonal growth following spinal cord injury. *Biomaterials,* 27(3), 443-451.

Szymańska, E., & Winnicka, K. (2015). Stability of Chitosan—A Challenge for Pharmaceutical and Biomedical Applications. *Marine Drugs,* 13(4), 1819.

Tao, J., Hu, Y., Wang, S., Zhang, J., Liu, X., Gou, Z., . . . Gou, M. (2017). A 3D-engineered porous conduit for peripheral nerve repair. *Scientific Reports,* 7, 46038.

Teng, S.-H., Wang, P., & Kim, H.-E. (2009). Blend fibers of chitosan–agarose by electrospinning. *Materials Letters,* 63(28), 2510-2512.

Thein-Han, W. W., & Misra, R. D. K. (2009). Biomimetic chitosan–nanohydroxyapatite composite scaffolds for bone tissue engineering. *Acta Biomaterialia,* 5(4), 1182-1197.

Tripathi, A., & Melo, J. S. (2015). Preparation of a sponge-like biocomposite agarose-chitosan scaffold with primary hepatocytes for establishing an in vitro 3D liver tissue model. *RSC Advances,* 5(39), 30701-30710.

Trivedi, T. J., Rao, K. S., & Kumar, A. (2014). Facile preparation of agarose-chitosan hybrid materials and nanocomposite ionogels using an ionic liquid via dissolution, regeneration and sol-gel transition. *Green Chemistry,* 16(1), 320-330.

Wan, Y., Wu, H., Yu, A., & Wen, D. (2006). Biodegradable Polylactide/Chitosan Blend Membranes. *Biomacromolecules, 7*(4), 1362-1372.

Yan, L.-P., Wang, Y.-J., Ren, L., Wu, G., Caridade, S. G., Fan, J.-B., . . . Reis, R. L. (2010). Genipin-cross-linked collagen/chitosan biomimetic scaffolds for articular cartilage tissue engineering applications. *Journal of Biomedical Materials Research Part A, 95A*(2), 465-475.

Yang, C., Gao, C., Wan, Y., Tang, T., Zhang, S., & Dai, K. (2011). Preparation and characterization of three-dimensional nanostructured macroporous bacterial cellulose/agarose scaffold for tissue engineering. *Journal of Porous Materials, 18*(5), 545-552.

Yin, Y., Ye, F., Cui, J., Zhang, F., Li, X., & Yao, K. (2003). Preparation and characterization of macroporous chitosan–gelatin/β-tricalcium phosphate composite scaffolds for bone tissue engineering. *Journal of Biomedical Materials Research Part A, 67A*(3), 844-855.

You, C., Li, Q., Wang, X., Wu, P., Ho, J. K., Jin, R., . . . Han, C. (2017). Silver nanoparticle loaded collagen/chitosan scaffolds promote wound healing via regulating fibroblast migration and macrophage activation. *Scientific Reports, 7*(1), 10489.

Zamora-Mora, V., Velasco, D., Hernández, R., Mijangos, C., & Kumacheva, E. (2014). Chitosan/agarose hydrogels: Cooperative properties and microfluidic preparation. *Carbohydrate Polymers, 111*(Supplement C), 348-355.

Zhu, J., & Marchant, R. E. (2011). Design properties of hydrogel tissue-engineering scaffolds. *Expert Review of Medical Devices, 8*(5), 607-626.